Journal of Applied Electrochemistry **29**: 1197–1203, 1999.

Effect of preparation conditions on the structure and catalytic activity of carbon-supported platinum for the electrooxidation of methanol

A. STOYANOVA, V. NAIDENOV, K. PETROV, I. NIKOLOV*, T. VITANOV and E. BUDEVSKI
Central Laboratory of Electrochemical Power Sources, Bulgarian Academy of Sciences Acad. G. Bonchev St., bl. 10 Sofia 1113, Bulgaria
(author for correspondence)*

Received 5 March 1997; accepted in revised form 24 February 1998

Key words: electrocatalysis, fuel cell, methanol

Abstract

Carbon-supported platinum catalysts (Pt/C) were prepared by treatment of PtO_2/C under different conditions: (a) heating at 380 °C in air, argon and hydrogen; (b) electrochemical reduction in H_2SO_4; and (c) reduction with $NaBH_4$. The effect of the preparation conditions on the structure and the catalytic activity of the catalysts for the electrooxidation of CH_3OH in acid media was studied. The highest activity was achieved for the catalyst treated in air. The activity is determined by the crystal faces exposed at the particle surface as well as particle size and the partial oxidation of the carbon support.

1. Introduction

The electrochemical oxidation of methanol in acid media is a subject of intensive research in the context of the development of the direct methanol fuel cell. The catalyst material most frequently used in this reaction is platinum. It is generally accepted that the rate determining step is the oxidation of the methanol adsorbate by the adsorbed OH species [1, 2]:

$$C-OH + OH_{ads} \longrightarrow CO_2 + 2\,H^+ + 2\,e^- \qquad (1)$$

The rate of Reaction 1 is determined by the coverage of the electrode surface with both the methanol adsorbate and hydrogen species. The efficiency of the Pt catalyst is improved if a well balanced coadsorption of methanol and water can be realized at low potential, where the methanol is adsorbed.

The Pt catalyst for electrooxidation of methanol in a fuel cell consists of carbon-supported Pt particles (Pt/C). The crystallite size effect of the Pt/C catalyst has been previously investigated [3–7]. The specific catalytic activity (SA) of Pt is thought to increase with particle size up to 4 nm and to remain constant above this size. The effect of the crystal faces exposed at the surface on the adsorption and catalytic behaviour of Pt with respect to CH_3OH electrooxidation has also been studied [8–11]. The face (1 1 0) was found to possess the highest activity [6, 10]. It was established that the adsorption of CH_3OH on platinized Pt proceeds more easily on sites strongly adsorbing H_2, the catalytic activity increasing with the number of sites [8, 9]. The effect of the nature of carbon surface groups on the catalytic activity was also demonstrated [7].

All the parameters determining the catalytic activity of Pt/C depend on the catalyst preparation conditions.

A comparatively simple method for preparation of Pt/C catalysts for electrooxidation of methanol is known [11]. This method is based on the deposition of fine oxides of platinum on carbon black in a Pt-salt solution and hydrogen peroxide followed by reduction with hydrogen at 280 °C. It was shown that the platinum surface is covered by chemisorbed oxygen, even at room temperature.

Considering the results obtained in [11], it is not yet clear to what extent the performance of carbon-supported Pt is influenced by the chemisorbed oxygen.

This work investigates the effect of the subsequent treatment of PtO_2/C, obtained according to [11] on the structure and catalytic activity of carbon-supported Pt for methanol oxidation.

2. Experimental details

2.1. *Catalyst preparation*

Carbon black (Vulcan XC-72, Cabot International), with a specific surface area (BET) of 290 $m^2\,g^{-1}$ was used as a support for all catalysts. The carbon-supported PtO_2 was prepared following the method of watanabe *et al.* [11]. Platinum Sulphite Acid sol. (E-TEK Inc.) was used. The dry PtO_2/C catalyst was treated as follows: (a) in air at 380 °C for 15 min (catalyst B_{380}–air), in argon (B_{380}–Ar)

and in hydrogen (B_{380}–H_2); (b) electrochemical reduction in H_2SO_4); (c) reduction with $NaBH_4$ (B_{NaBH_4}).

It is assumed that the following processes take place during heating in air:

$$C + \tfrac{1}{2}O_2 \longrightarrow CO \quad (2)$$

$$PtO_2 + 2\,CO \longrightarrow Pt + 2\,CO_2 \quad (3)$$

$$PTO_2 + C \longrightarrow Pt + CO_2 \quad (4)$$

As a result a decrease of 20–25% of the sample weight and an increase of 12.5–13% of the metallic Pt content, respectively, was observed. In the case of Ar atmosphere the corresponding figures are 12–13% and 11.5%, respectively. The greater decrease in the sample weight as compared to the theoretical value of ~2% is most probably due to the presence of a small amount of oxygen (~50 ppm) in the argon, which makes it possible for Reactions 2 and 3 to proceed. No change in the sample weight was observed after heating in H_2.

The electrochemical reduction was performed by passing the theoretical quantity of electricity to reduce the sample at a constant potential of $E = 20$ mV (RHE) in 0.5 M H_2SO_4. The chemical reduction of PtO_2/C was performed in 0.5% solution of $NaBH_4$.

X-ray diffraction patterns were obtained using a PHILIPS PW 1730 diffractometer equipped with a PW 1710 automatic step scanning system and a diffracted-beam curved graphic monochromator. Intensity measurements were made at intervals of 0.05° over 2Θ range 30°–90° using CuK_2 radiation and a step counting time of 2 s. The mean size of Pt crystallites in the catalyst samples were determined from the Sherrer equation [12] by comparing the values of peak width calculated at constant 2Θ value of 69°. In some spectra the peak was necessarily treated as consisting of two peaks located at the same angle but having different widths, thus representing two characteristic sizes of particles. The average size in such cases was roughly estimated as a mean of two sizes measured from the integral intensities of respective peaks.

2.2. *Electrode preparation*

The electrodes (2 cm^2) were prepared by pressing a mixture of the catalyst with 20 w/o Teflon (Hosteflon TF 3542) on both sides of a stainless steel screen at 320 °C and at a pressure of 300 kg cm^{-2} for 2 min. The amount of the catalyst in the electrodes was 10 mg cm^{-2}. To prevent the screen from corrosion the latter was covered beforehand with a Teflon acetylene black composite binder (XC).

2.3. *Catalyst characterizing*

Pt/C electrodes were characterised by cyclic voltammetry using a computer-controlled Solartron 1286 potentiostat. Cyclic voltammetric scans were obtained in argon saturated 0.5 M H_2SO_4 in the potential range from +0.02 to +0.350 V vs RHE at a scan rate of 10 mV s^{-1}. A Hg/Hg_2SO_4 reference electrode in 0.5 M H_2SO_4 was used; the potential was referred to the RHE in the same solution. Platinum specific surface ares $S/m^2\,g^{-1}$ was determined from the hydrogen desorption area in the anodic voltammograms assuming that 1 cm^2 of smooth Pt requires 210 μC [13]. The average size of the Pt particles was determined from the relation [14]:

$$\bar{d} = \frac{6 \times 10^3}{S\rho} \quad (5)$$

where ρ is density of Pt (21.45 g cm^{-3}).

The stability of the catalysts was determined by cycling the electrodes in the potential range from +0.020 to +0.350 V vs RHE where modification of the catalyst surface takes place [15].

The galvanostatic current–potential curves of methanol oxidation were obtained in argon saturated 1 M CH_3OH + 0.5 M H_2SO_4 using a Tacussel Bl-PAD potentiostat. A three electrode cell with a Pt counter electrode and a Hg/Hg_2SO_4 reference electrode were used. The electrocatalytic activity of the catalysts was expressed as the steady state current density at +0.550 V vs RHE in the Tafel region. The activities were normalized per unit real surface area of Pt specific activity (SA) and per mg catalyst-mass ac tivity (MA).

3. Results and discussion

3.1. *XRD results*

XRD spectra of catalysts subjected to various treatments are presented in Fig. 1. The spectrum of the catalysts as prepared and after chemical reduction with $NaBH_4$ is identical to that of the Vulcan XC-72 which suggests the presence of amorphous Pt, PtO_x phases only. Crystallites of Pt appear to grow after any of the treatments used and a summary of their dimensions is given in Table 1. A monodispersed distribution of 2–4 nm was obtained after electrochemical reduction in H_2SO_4, whereas bidispersed particles with original 2–4 nm and 15–20 nm size are produced during heat treatment in different atmospheres. The large crystallites seem to be formed by fusion of particles originally deposited as aggregates onto the catalyst support.

The systematic decrease of the peak height of active carbon at 43° after heat treatment is probably due to the oxidation of Pt promoted by oxygen originating either from PtO_x in H_2 or Ar atmosphere, or from air.

3.2. *Electrochemical characterization*

Figure 2 presents the cyclic voltammograms, initial and after 50 cycles, in 0.5 M H_2SO_4 for four of the investigated samples. It can be seen that the original catalysts differ in structure:

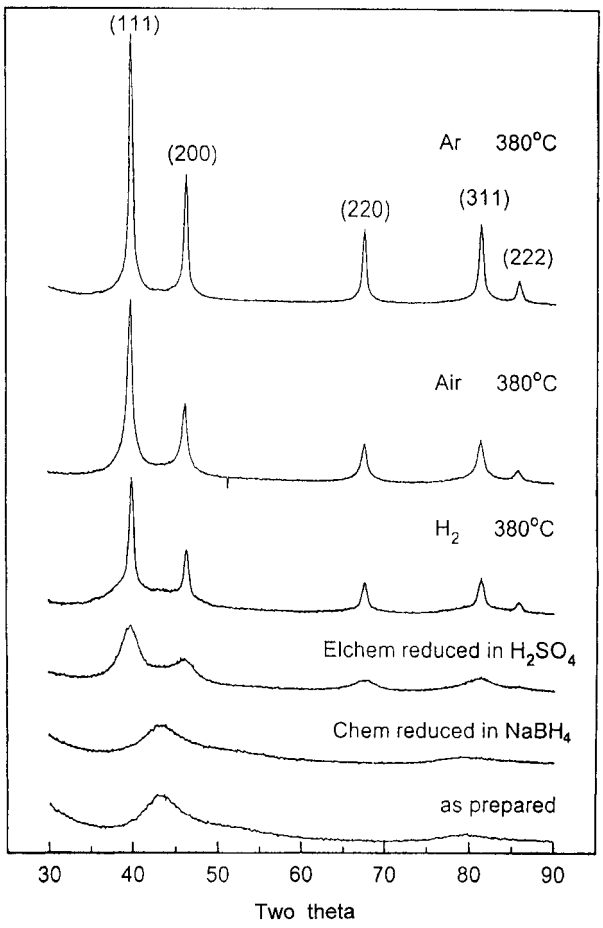

Fig. 1. XRD pattern of PtO_2/C as prepared and Pt/C catalyst prepared at different conditions.

(i) The anodic hydrogen desorption regions in the voltammograms of the sample heated in H_2 and Ar, as well as of the sample subjected to electrochemical reduction feature peaks, though not well pronounced, of weakly bound hydrogen (Pw-crystal face (1 1 1)), medium bound hydrogen (Pm-crystal face (1 1 0)) and strongly bound hydrogen (Ps-crystal face (1 0 0)) [15], where as Pw is missing in the curve for the sample heated in air.

(ii) The ratio between the peak heights hp_s and hp_w normalized against a unit electrochemical surface area, hp_s/hp_w, differs for the first three samples, but is greater than 1 in all three cases.

(iii) A comparison between the oxidation-reduction peaks of the Pt surface shows that there is only one well pronounced cathodic peak at $+0.6$ V in the curves for samples heated in H_2 and for the electrochemically reduced one, whereas for the sample heated in Ar there is a hint of another peak at $+0.75$ V. In the cyclic voltammograms for the sample heated in air the peaks at $+0.6$ V and at $+0.75$ V merge forming a plateau.

After 50 cycles the following changes are observed:

(i) The peak for the weakly adsorbed hydrogen in the anodic desorption region of the voltammogram is well pronounced for all samples, whereas the potential region between $+0.1$ and $+0.3$ V, where the peaks for the medium and strongly bound hydrogen are to be found, features a plateau.

(ii) For the sample heated in Ar and H_2 atmosphere and the electrochemically reduced one the height of the hp_w peak exceeds that of the plateau, whereas for the sample heated in air both heights are equal.

(iii) The oxidation–reduction peaks are transformed into a plateau between $+0.6$ V and at $+0.75$ V for all four samples.

The effect of repeated potential cycling on the specific surface area (S), average particle size ($\bar{d}$), calculated by Equation 5 and the peak height (hp_s) is presented in Table 2.

The values of $\bar{d}$ determined by XRD (Table 1) and electrochemically (Table 2) are nearly the same except for the sample prepared in H_2, where, most probably, an amorphous phase has been formed. All the catalysts prepared by heating contain two types of particles: the initially obtained particles which are small in size, and the large ones, consisting of aggregates of small particles.

The largest specific surface area is exhibited by the sample B_{380}–H_2 while the smallest one is for sample B_{380}–air. Similar results have been obtained in the same conditions by Enyo et al. [17].

An increase in peak height, hp_s, normalized per unit surface area, with the particle size is observed. This result is in good agreement with the finding of Kinoshita [18] that the surface averaged distribution of Pt(1 0 0) increases with $\bar{d}$. A similar surface distribution has also been found for Pt(1 1 1) [18]. As can be seen in Fig. 2, however, such a face was not revealed for the catalyst with largest particle size heated in air. According to the same author the number of adsorption sites on the faces (1 0 0), (1 1 1) and (1 1 0) of Pt are 4, 3 and 5, respectively. This means that, for methanol oxidation with Reaction 1 as rate determining step, the faces (1 0 0) and (1 1 0) are favourable.

The appearance of an oxidation–reduction peak at $+0.75$ V for the sample with largest average particle size heated in air (Fig. 2) is in good agreement with the finding that Pt particle are more easily reduced when d increases [7, 19]. The oxidation of the sample with small particles reaches maximum at a potential of 50 mV more cathodic than that of the sample heated in air.

After cycling a decrease in both the catalyst surface area and the ratio hp_s/hp_w was observed; the larger the

Table 1. Particle size determined by XRD

Catalyst	Size, d /nm	Average size, $\bar{d}$ /nm
B_{380}–air	3.4, 15	8.6
B_{380}–Ar	3.7, 21	7.8
B_{380}–H_2	1.8, 14	9.2
$B_{H_2SO_4}$	2.4–4.4	3.5

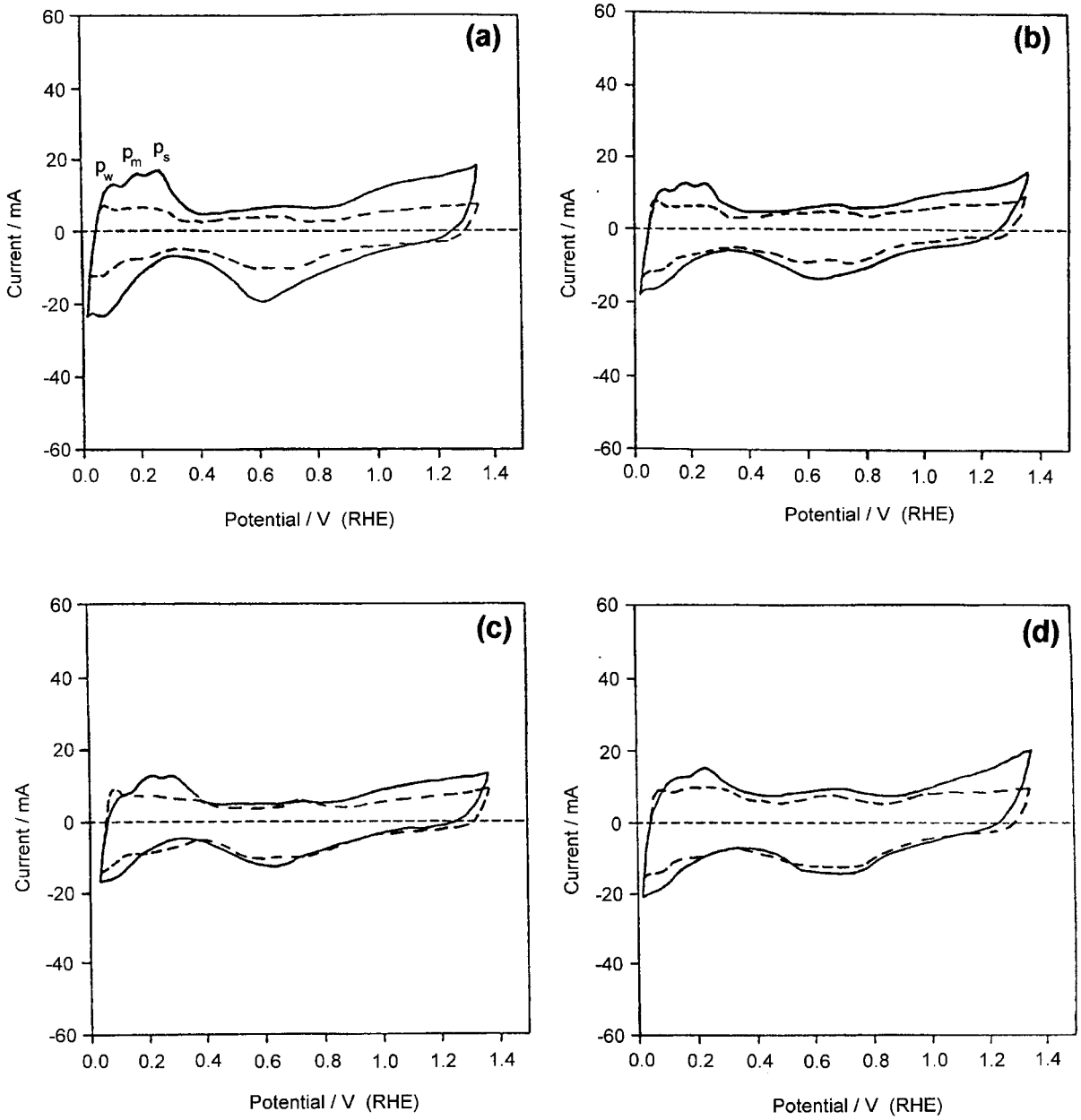

Fig. 2. Cyclic voltammograms of catalysts in argon saturated 0.5 M H_2SO_4. Scan rate 10 mV s^{-1}; full line – scan 2; dotted line – scan 50; (a) B_{380}–H_2; (b) B_{380}–Ar; (c) $B_{H_2SO_4}$; (d) B_{380}–air.

initial surface area, the less stable the sample. The most stable in this respect appeared to be the sample treated in air. A similar effect was described earlier [15].

An increase in d was also observed after cycling. The latter has an effect on the oxidation–reduction peaks, which results in easier reduction of the surface.

Table 2. Effect of the repeated potential cycling on the specific surface area (S), average particle size ($\bar{d}$) and peak height (hp_s) of the investigated catalysts

Catalyst	2 cycles				20 cycles		50 cycles		
	S /$m^2\ g^{-1}$	$\bar{d}$ /nm	hp_s/S /$\mu A\ cm^{-2}$	hp_s/hp_w	S /$m^2\ g^{-1}$	$\bar{d}$ /nm	S /$m^2\ g^{-1}$	$\bar{d}$ /nm	hp_s/hp_w
B_{380}–air	33.5	8.4	11.3	–	35.4	12.0	21.9	12.8	2.3
B_{380}–Ar	42.9	6.5	10.1	1.36	40.0	7.0	27.8	10.0	0.83
B_{380}–H_2	68.4	4.1	9.8	1.49	49.0	5.7	29.8	9.4	0.95
$B_{H_2SO_4}$	52.7	5.3	9.2	4.75	30.1	9.3	27.2	10.3	0.74

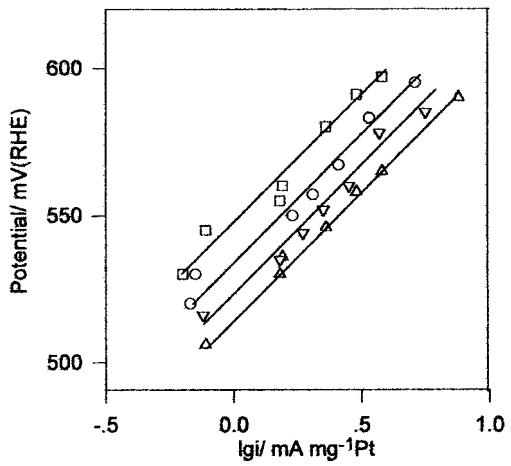

Fig. 3. Tafel plots of oxidation of 1 M CH_3OH in 0.5 M H_2SO_4 on electrodes with different catalysts: Key: (○) B_{380}–H_2; (□) $B_{H_2SO_4}$; (△) B_{380}–Ar; (▽) B_{380}–air.

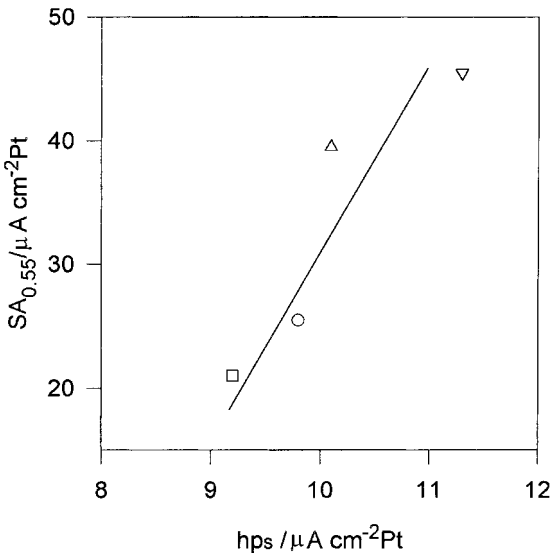

Fig. 4. Specific activity of the catalysts against the peak height hp_s in 1 M CH_3OH + 0.5 M H_2SO_4 at $E = +0.55$ V. Key: (□) $B_{H_2SO_4}$; (○) B_{380}–H_2; (△) B_{380}–Ar; (▽) B_{380}–air.

3.3. *Electrooxidation of methanol*

The E vs log i plots of the catalyst studied in 1 M CH_3OH + 0.5 M H_2SO_4 are presented in Fig. 3. Tafel slopes of 110–130 mV dec.$^{-1}$, close to the theoretical, were observed for all the samples.

The values of the Tafel slopes, the mass activity and the specific activity after 2 and 50 cycles are presented in Table 3. Because of the very small activity of the samples treated chemically with $NaBH_4$ the corresponding values are not included in the table.

It is seen from Table 3 that after 2 cycles the greatest specific activity is exhibited by the sample B_{380}–air while the greatest mass activity is for the sample B_{380}–H_2. The juxtaposition of SA with the average size $\bar{d}$ determined electrochemically (Table 2) shows an increase in SA with $\bar{d}$. This result disagrees with other data. According to van Veen *et al.* [7] SA does not depend on the particle size for $d > 4$ nm, while no dependence between SA and $\bar{d}$ has been observed by Enyo et al. [17].

The relationship observed between SA and $\bar{d}$ is probably due to the different crystallographic structure of Pt particles, which is backed up by both the linear dependence between SA and the peak heights of the differently bonded hydrogen, h_{ps} (Fig. 4) and $h_{ps} + h_{pm}$ (Fig. 5), respectively.

Other factors responsible for the increase in SA with $\bar{d}$ could be the reduction of Pt–O taking place on larger particles and/or the oxidation of C in air and, probably, in Ar. According to van Veen [7] the last effect results in an increase in catalytic activity of Pt/C with respect to methanol oxidation. Thus, it appears that the different specific activity of the catalysts is determined by at least three factors: particle size, crystal faces exposed at the particle surface and oxidation state of the carbon support. The greatest specific activity of the sample prepared in air is most probably due to all the factors mentioned.

After cycling the electrodes, as also pointed out in [9], the specific activity increases. The increase is highest for the samples prepared in H_2 and after electrochemical reduction and least for that prepared in Ar (Table 3). It is also known that, during cycling, dissolution of the small thermodynamically unstable particles takes place [14] and catalytic activity for methanol oxidation increases proportionally to the particle size up to 4.5 nm [7].

In explaining these effects cyclic voltammograms were used (Fig. 2).

After cycling a well pronounced peak of the weak-bonded hydrogen is seen which allows the areas corresponding to both the strong and the medium bonded adsorbed hydrogen, $S_{ps} + S_{pm}$, to be determined. The quantity

Table 3. Tafel slope (b), mass activity (MA) and specific activity (SA) of the catalysts Pt/C after different number of cycles

Catalyst	2 cycles			50 cycles		
	MA /mA mg^{-1} Pt	b /mV dec^{-1}	SA /μA cm^{-2} Pt	MA /mA mg^{-1} Pt	b /mV dec^{-1}	SA /μA cm^{-2} Pt
B_{380}–air	1.54	125	4.60	1.42	130	6.52
B_{380}–Ar	1.70	124	4.00	1.09	120	4.21
B_{380}–H_2	1.80	125	2.63	1.73	115	5.80
$B_{H_2SO_4}$	1.2	123	2.28	1.17	120	4.30

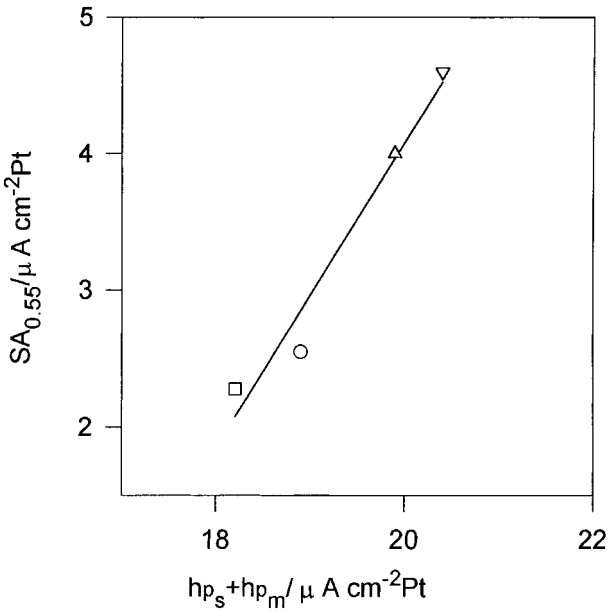

Fig. 5. Specific activity of the catalysts against the peak heights $hp_m + hp_s$ in 1 M CH_3OH + 0.5 M H_2SO_4 at $E = +0.55$ V. Key: (□) $B_{H_2SO_4}$; (○) B_{380}–H_2; (△) B_{380}–Ar; (▽) B_{380}–air.

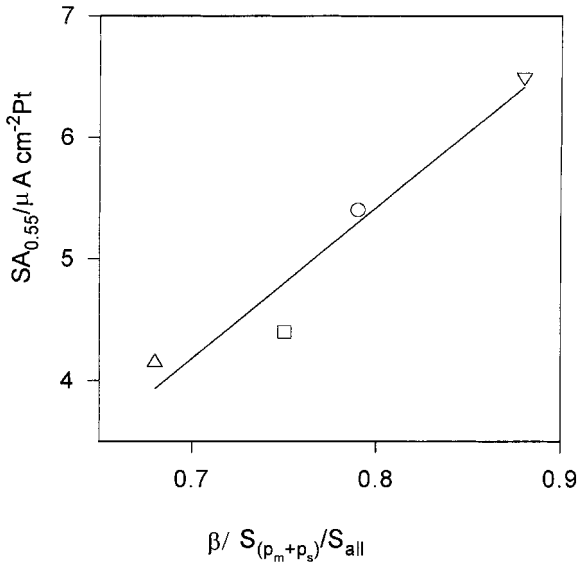

Fig. 6. Dependence of the specific activity of the catalysts on β in 1 M CH_3OH + 0.5 M H_2SO_4 at $E = +0.55$ V. Key: (△) B_{380}–Ar; (□) $B_{H_2SO_4}$; (○) B_{380}–H_2; (▽) B_{380}–air.

$$\beta = \frac{S(p_m + p_s)}{S_{tot}} \tag{6}$$

is introduced. (S_{tot}, total surface area). Figure 6 shows the relationship between the specific activity and β after cycling. It is evident that because of the dissolution of the small particles the specific activity is mainly determined by the crystallographic structure.

From the data presented it appears that the catalyst prepared in air exhibits the greatest specific activity and stability but its mass activity is smaller as compared to the catalyst treated in H_2 because of the larger surface area of the latter. This leads to the idea that a catalyst better than that heated in H_2 could be obtained in air from starting material comprising smaller PtO_2 particles.

A highly dispersed PtO_2 was obtained by addition of H_2O_2 to a concentrated platinum sulphite acid solution. The subsequent steps are as described in [11]. The physical and electrochemical characteristics of the catalyst thus prepared, and subsequently treated in air at 380 °C, are given in Table 4.

Comparison of the data in Table 4 with those in Tables 2 and 3 shows that the catalyst with a particle size $\bar{d} = 5.7$ nm exhibits a greater mass activity in comparison with the same catalyst with $\bar{d} = 8.4$ nm as well as with that prepared in hydrogen with $\bar{d} = 4.1$ nm.

An attempt was made to improve the mass activity by heating in hydrogen a PtO_2/C sample with smaller particles and larger specific surface area, respectively. The catalyst obtained gives $S = 104\,m^2\,g^{-1}$ and $\bar{d} = 2.7$ nm, but due to the small specific activity, $SA = 1.6\,\mu A\,cm^{-2}$ Pt, its mass activity is only 1.7 mA mg^{-1} Pt.

It is of interest to compare the initial mass activities of the catalysts E-TEK Inc., Pt–Ru/C prepared in [11] and that obtained in this work. The result obtained with electrodes prepared as described in Section 2.2. are as follows: 0.57 mA mg^{-1} Pt for the catalyst promoted with 10 wt % Pt/C (E-TEK, Inc.) and 3.85 mA mg^{-1} Pt for that with 26 wt % Pt–Ru/C. It is seen that the mass activity of the Pt/C catalyst prepared in this work considerably exceeds that of the commercial one but is smaller than that of the Pt–Ru/C catalyst.

4. Conclusion

The catalytic activity of the catalyst synthesized from PtO_2/C for the electrooxidation of methanol in acid media depends on the reduction conditions of PtO_2:

Table 4. Surface area (S), average particle size ($\bar{d}$) mass activity (MA) and specific activity (SA) of the catalyst B_{380}–air after different number of cycles

Catalyst	2 cycles				50 cycles			
	S /$m^2\,g^{-1}$	$\bar{d}$ /nm	MA /mA mg^{-1}	SA /$\mu A\,cm^{-2}$ Pt	S /$m^2\,g^{-1}$	$\bar{d}$ /nm	MA /mA mg^{-1}	SA /$\mu A\,cm^{-2}$ Pt
B_{380}–air	48.7	5.7	2.31	4.74	36.6	7.64	2.02	5.52

electrochemical, chemical with $NaBH_4$ and thermal treating at 380 °C in air, argon and hydrogen. The greatest activity is exhibited by the catalyst prepared in air. The activity is determined by the crystal faces exposed at the particle surface as well as the particle size and the partial oxidation of the carbon support.

References

1. V.S. Bagotzky and Ju. B. Vassilyev, *Electrochim. Acta* **12** (1967) 1323.
2. B.D. McNicol, *J. Electroanal. Chem.* **118** (1981) 71.
3. P.A. Attwood, B.D. Mc. Nicol and R.T. Short, *J. Appl. Electrochem.* **10** (1980) 213.
4. M. Enyo, K. Machida, A. Fukuoka and M. Ichikawa, *in* 'Electrochemistry in Transition' (edited by O. J. Murphy), Plenum, New York, pp. 359–369.
5. M. Watanabe, S. Saegusa and P. Stonehart, *J. Electroanal. Chem.* **271** (1989) 213.
6. K. Jakikozawa, J. Fuiji, J. Matsuda, K. Nishimura and J. Takasu, *Electrochim. Acta* **36** (1991) 973.
7. T. Frelink, W. Visser and J.A.R. van Veen, *J. Electoanal. Chem.* **382** (1995) 65.
8. B. Beden, F. Kadigran, C. Zamy and J.M. Zeger, *ibid.* **142** (1982) 171.
9. T. Frelink, W. Visser and J.A.R. van Veen, in press.
10. S. Motoo and N. Furuya, Kinzoku Hyomen Gijyutsu, *J. Surf. Finish. Metals* **36** (1985) 386.
11. M. Watanabe, M. Uchida and S. Motoo, *J. Electroanal. Chem.* **229** (1987) 395.
12. H.P. Klug and Z.E. Alexander, 'X-ray Diffraction Procedures for Polycristalline and Amorphous Materials', J. Wiley & Sons, New York, (1974).
13. T. Biegler, D.A.J. Rand and R. Woods, *J. Electroanal. Chem.* **29** (1973) 269.
14. O. Stonehart, *J. Appl. Electrochem.* **22** (1992) 995.
15. K. Kinoshita, J.T. Zuindquist and O. Stonehart, *J. Electroanal. Chem.* **48** (1973) 157
16. F.G. Will, *J. Electrochem. Soc.* **112** (1965) 451.
17. P.C. Buswas, J. Nodasaka and M. Enyo, *J. Appl. Electrochem.* **26** (1996) 30.
18. K. Kinoshita, *J. Electrochem. Soc.* **137** (1996) 845.
19. J. Takasu, J. Fuiji, K. Jasuda, J. Iwanaga and J. Matsuda, *Electrochim. Acta* **34** (1989) 453.